UDC 681.51:[004.896:004.438]
DOI https://doi.org/10.32782/2663-5941/2025.5.2/26

***Nevliudov I.Sh.***
Kharkiv National University of Radio Electronics

***Yevsieiev V.V.***
Kharkiv National University of Radio Electronics

***Jabrayilzade E.A.***
Kharkiv National University of Radio Electronics

# NUMERICAL SIMULATION OF DC MOTORS ROTATION SPEED IN COLLABORATIVE ROBOTS USING ADAPTIVE NEURAL PID CONTROLLER

*A method for controlling the speed of DC motors of a collaborative robot using Adaptive Neural PID controllers is considered in the article. It combines the classical theory of automatic control with artificial intelligence methods. The purpose of the study is to create a mathematical model and software implementation of an adaptive neural controller for stabilizing the speed of the RS540 motor with feedback from the HC-020K speed sensor.*

*The object of analysis is the "motor-sensor-controller" system, for which transfer functions, structural diagrams and stability studies based on the Nyquist criterion are constructed. The scientific novelty is the use of an adaptive neural network for dynamic tuning of PID controller coefficients* $(K_p, K_i, K_d)$*, which provides better stability and minimum control time in conditions of disturbances and sensor noise. Conclusions: during numerical simulation, it was found that the evolution of PID coefficients allows the system to adapt independently: after the initial impulse* $K_d$ *overload, the value decreases from 100 to a stable 0–2, while* $K_p, K_i$ *remaining within the range of 0.5–2.0, which indicates a balance between speed and elimination of static error. The transient characteristic showed that in the presence of high-frequency noise from the HC-020K sensor, the true motor speed* $w_{true}$ *stabilizes in the range of ±40 rad/s, while the measured speed* $w_{meas}$ *fluctuates up to ±150 rad/s, confirming the need for filtering. Analysis of the control signals revealed actuator saturation, but the adaptive network reduced the pulse amplitude and ensured no instability. Using the Nyquist criterion showed a phase margin of more than 45° and an amplitude margin of more than 6 dB, confirming the reliable operation of the system. The results obtained prove that the proposed method allows reducing the control time to 0.2–0.3 s and ensures the stability of the manipulative collaborative robot even in difficult production conditions.*

***Key words:*** *DC motor RS540, HC-020K, Adaptive Neural PID, collaborative robot, system stability, Nyquist criterion, speed control, neural network, actuator.*

**Formulation of the problem.** The relevance of researching a method for controlling the rotational speed of DC motors in collaborative robots using Adaptive Neural PID controllers is determined by current trends in the development of Industry 5.0 [1-3], where robotic systems must ensure high precision, reliability, and safe interaction with humans. Classic PID controllers, widely used in industry, have limitations when working with nonlinear objects and systems with variable parameters, such as collaborative mobile robots [4-7]. In such conditions, load fluctuations, sensor noise signals, and dynamic disturbances lead to a decrease in control accuracy and deterioration of system stability. The problem lies in the inability to effectively ensure optimal control time and minimal error solely through static controller coefficients [8-10]. This is why there is a need for intelligent adaptation methods capable of changing control parameters in real time depending on operating conditions. Adaptive Neural PID controllers combine the advantages of classical automatic control theory with neural networks, which allows for the nonlinearities of the object to be taken into account, the influence of sensor noise, such as HC-020K, to be compensated for, and the accuracy of stabilizing the speed of the RS540 DC motor to be increased [11-13]. Thus, the research is aimed at solving the problem of ensuring the stability and high performance of collab-

orative robots in dynamic production environments, which emphasizes its practical significance and scientific novelty.

**Analysis of recent studies and publications.** The article by R. Tiwari, A. Srinivaas, and others proposes adaptive navigation of collaborative robots based on reinforcement learning with sensor fusion, which increases resistance to noise and environmental dynamics [14]. For our topic, this is useful as a high-level trajectory planning strategy that can be combined with low-level AN-PID speed control, but the parameters of the DC drive's electromechanics are not directly identified there. Y. Wang's work presents the theory and practice of PID control of DC motors in all-terrain robots, including simulation and tuning of controllers and issues of saturation and limitations [15]. This directly feeds into our RS540 model and sets the basic $K_p$-$K_i$-$K_d$ ranges, but does not solve real-time adaptation, which we cover with a neural network. In their article, X. Zhao and Y. Song developed velocity-free neuro-adaptive cooperative control with adjustable performance constraints for two-armed robots [16]. This approach confirms the effectiveness of neuroadaptation for compensating for uncertainties and can be used as a methodological guideline for forming the AN-PID learning law; direct application requires simplification, as we measure speed and single-axis drive. The publication by W. Chen, Y. Jing, and others presents distributed navigation based on AE-KF integrated GNSS/INS positioning with MPC [17]. For our task, this is useful at the level of filtering and planning, in particular the idea of combining state estimation and optimization, but this stack does not solve the motor speed control and does not contain a speed loop. The research by Z. Liu, O. Zhang, and others proposes adaptive neural fixed-time control for robots with input saturation and specified accuracy [18]. The results are relevant to our case because they take into account saturations and guarantee convergence in a limited time; we can use them to select the structure of barrier functions in the AN-PID stability supervisor. The work of N. Terras, F. Pereira, and others integrates deep learning computer vision systems into real-time cobot scenarios [19]. This is useful for high-level perception and assessment of safe zones, but does not provide recipes for tuning the drive speed loop. The article by K. Peta, M. Wiśniewski, and others compares single- and dual-arm cooperative platforms in precision assembly, highlighting the requirements for dynamics and smoothness of motion [20]. From this, we take the requirements for control time and speed fluctuations, although the motor control methods are not detailed there. The publication by L. Gargioni, D. Fogli, and others describes a hybrid approach to EUD programming of robots for personalized medical preparations [21]. The relevance lies in the requirements for safe interaction and adaptability, but in the speed control loop, this is indirect and cannot be used directly. The report by S. Sukhorukov and M. Lyamin proposes a methodology for implementing some collaborative functions in industrial robots [22]. We can use their recommendations for integrating safe modes and speed limits, but the specifics of DC motors and neural adaptation are not disclosed there. Finally, in the work of I. Nevliudov, V. Yevsieiev, and others, mathematical support for adaptive control of intelligent manipulator gripping has been developed [23]. This confirms the feasibility of adaptive laws in collaborative nodes and can be transferred to our AN-PID as an approach to online parameter identification, although the control object is different. In summary, the analysis shows the high relevance of combining a classical speed loop with neuroadaptation for DC drives of collaborative robots: the literature provides a foundation for sensor fusion, navigation, saturation handling, and convergence guarantees, while our work fills the niche of low-level RS540 speed control with real sensors, ensuring stability, speed, and robustness in dynamic conditions.

**Task statement.** The purpose of the article is to develop a mathematical model and software implementation for numerical simulation of an adaptive neural controller for stabilizing the speed of the RS540 motor with feedback from the HC-020K speed sensor in the control system for moving a model of a wheeled mobile robot manipulator.

When developing experimental models of collaborative manipulative mobile robots, precise control of the rotation speed of DC motors is important for smooth movement, synchronization with the manipulator, and safe interaction with humans [24, 25]. Classic PID controllers often do not provide adequate accuracy under variable loads and nonlinear motor characteristics. The use of Adaptive Neural Control (ANC) allows you to automatically adapt control parameters to changes in system dynamics and achieve stability even under uncertainties [26, 27].

Let's develop a block diagram of automatic speed control of the DC Motor RS540 [28] with Adaptive Neural Control (ANC) for selecting PID coefficients in real time, which is shown in Figure 1.

Let's describe the signals (input/output/internal) and parameters shown in Fig. 1:

$w_{ref}$ – set angular velocity [rad/s], system input (setpoint);

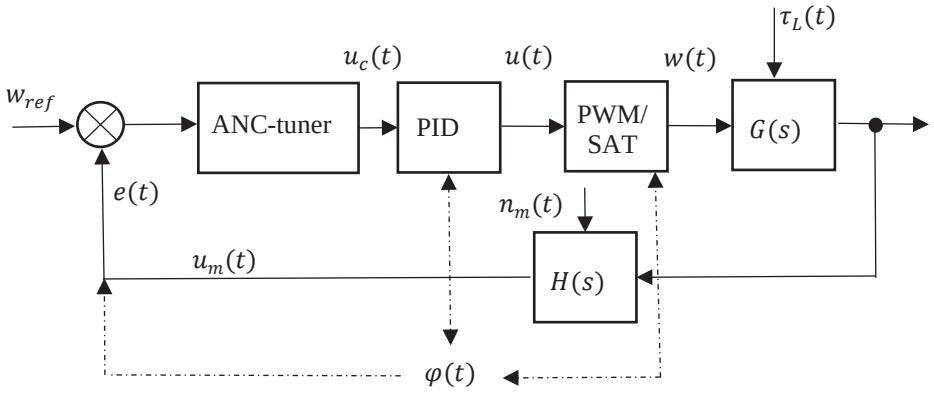


**Fig. 1. Block diagram of automatic speed control of DC Motor RS540 with Adaptive Neural Control (ANC) for real-time selection of PID coefficients**

$w(t)$ – actual angular velocity of the rotor [rad/s], object output;

$w_m(t)$ – measured velocity [rad/s] after HC-020K, feedback;

$e(t)$ – tracking error [rad/s], internal signal in the summing circuit;

$u_c(t)$ – "raw" PID control [V or rel. PWM], internal;

$u(t)$ – saturated control (driver/power supply limitations taken into account), object input;

$\theta(t)=\{K_p, K_i, K_d\}$ – adaptive PID coefficients, internal ANC-tuner output;

$\varphi(t)$ – feature vector at the neural network input;

$\tau_L(t)$ – load disturbance torque [N·m];

$n_m(t)$ – sensor measurement/quantization noise, disturbance in the measurement channel.

Let's look at the sequence of how the DC Motor RS540 speed control counter with Adaptive Neural Control (ANC) works to select PID coefficients in real time (Fig. 1):

1. The operator or planner sets $w_{ref}$;

2. The error $e$ forms the input to both the PID and the ANC tuner;

3. The neural network $\varphi(t)$ calculates PID parameters that minimize instantaneous/forecast error, taking into account constraints and robustness;

4. PID generates $u_c$, saturation/PWM block forms physically permissible $u$;

5. The motor $G(s)$ reacts to $u$ and the disturbance $\tau_L$, the HC-020K sensor turns $w_m$;

6. Feedback closes the loop, ensuring tracking and adaptation when load/parameters change.

The mathematical model of the DC Motor RS540 in transfer form between input voltage $u(t)$ and angular velocity $w(t)$ will be as follows:

$$J\frac{dw(t)}{dt}+Bw(t)=K_t i(t)$$
$$L\frac{di(t)}{dt}+Ri(t)=u(t)-K_e w(t) \quad (1)$$

Where: $J$ – rotor inertia moment [kg·m²]; $B$ – viscous friction coefficient [N·m·s]; $R$ – winding resistance [Ohm]; $L$ – winding inductance [Hn]; $K_t$ – torque coefficient [N·m/A]; $K_e$ – back EMF coefficient [V·s/rad].

Transfer function between input voltage $U(s)$ and angular velocity $\Omega(s)$:

$$G(s)=\frac{\Omega(s)}{U(s)}=\frac{K_t}{(JL)s^2+(JR+BL)s+(BR+K_tK_e)} \quad (2)$$

HC-020K speed sensor, this module gives a pulse signal corresponding to the rotation speed. Accordingly, we will receive a speed signal $w_m(t)$ after processing using the frequency method:

$$w_m(t)=k_s\cdot f_{imp}(t) \quad (3)$$

Where: $w_m(t)$ – the measured instantaneous value of the angular velocity of the motor [rad/s or rpm], which is the output signal of the sensor after conversion. It is used in the control system for comparison with the reference signal; $f_{imp}(t)$ – Pulse frequency [Hz] generated by the HC-020K sensor output based on the rotation of the motor shaft. Each motor rotation corresponds to a certain number of pulses (depending on the encoder design); $k_s$ – scaling factor [rad/s per 1 Hz or rpm per 1 Hz], which reflects the relationship between the sensor pulse frequency and the actual shaft rotation speed. It depends on the number of pulses per revolution of the encoder (PPR – pulses per revolution) and the selected unit system.

The HC-020K sensor [29] converts mechanical motion (motor rotation speed) into a digital pulse sequence. The faster the shaft rotates, the higher the signal frequency. Mathematical model 3 shows that the measured speed

is directly proportional to the frequency of these pulses, and the coefficient $k_s$ performs the function of converting pulses into physical units of speed.

Adaptive Neural PID (ANC) control method, based on the principle of using a neural network for adaptive real-time tuning of $K_p, K_i, K_d$. Classic form of PID controller:

$$u(t) = K_p e(t) + K_i \int e(t)dt + K_d \frac{de(t)}{dt} \quad (4)$$

Where: $e(t) = w_{ref}(t) - w_m(t)$

Adaptive neural network adjusts parameters:

$$\left[K_p, K_i, K_d\right] = f_\theta(e(t), \dot{e}(t), \int e(t)dt) \quad (5)$$

Where: $K_p$ – proportional coefficient, which determines the strength of the controller's response to an instantaneous error $e(t)$ and is responsible for the speed of the system's response; $K_i$ – integral coefficient, which accumulates the error over time $\int e(t)dt$ and eliminates the steady-state error in the set mode; $K_d$ a differential coefficient that takes into account the rate of change of the error $\dot{e}(t)$ and suppresses system oscillations; $e(t)$ – current error between the set speed and the measured speed from the HC-020K sensor; $\dot{e}(t)$ – error derivative, showing the trend of change (whether the deviation is increasing or decreasing); $\int e(t)dt$ – error integral, characterizing the accumulated deviation over a certain time; $f_\theta(\cdot)$ – a representation implemented by a neural network with parameters $\theta$ (weights and offsets), which calculates optimal values $\left[K_p, K_i, K_d\right]$ based on input signals, providing adaptability and real-time learning.

Thus, model 5 means that the system automatically selects the PID controller parameters depending on the error dynamics. This allows for compensation for the nonlinearities of the RS540 motor, load changes, and environmental instabilities, which is critical for a collaborative mobile manipulator robot.

Verification of the stability of the system according to the Nyquist criterion [30] is performed for the transfer function of the open-loop system:

$$L(s) = G(s) \cdot G_c(s) \quad (6)$$

Where: $G(s)$ – transfer function of the control object (in our case, the RS540 DC motor with the HC-020K sensor). It describes the dynamics of the physical system: how a change in the input signal (voltage on the motor) is converted into an output signal (angular velocity). It looks like this:

$$G(s) = \frac{K}{Ts+1} \quad (7)$$

Where: $K$ – object gain factor; $T$ – engine idle time.

$G_c(s)$ – transfer function of the controller, in our case Adaptive Neural Control PID). It sets the control law for the system:

$$G_c(s) = K_p + \frac{K_i}{s} + K_d s \quad (8)$$

Where: $K_p, K_i, K_d$ – coefficients of proportional, integral, and differential components that determine the system's response to error;

$L(s)$ – general open-loop transfer function. It describes how the system responds to an input signal without taking feedback into account. It is for this function that a Nyquist plot is constructed, which allows the stability of a closed-loop system to be assessed.

ANC-tuner (neural network PID adapter) generates:

$$\theta(t) = \{K_p(t), K_i(t), K_d(t)\} = f_\Theta(\varphi(t)) \quad (9)$$

Where: $\varphi(t) = [e, \dot{e}, \int e, w_m, u, \text{additional context variables}]^T$ – feature vector, $\Theta$ – NM weights (adapted online by law $\dot{\Theta} = -\eta\, \partial \mathcal{L}/\partial \Theta$ or by the gradient of the Lyapunov stabilizing functional).

Actuator/saturation (PWM/SAT, Robot HAT) (see Fig. 1) $u(t)$ – converts the control voltage/command into PWM:

$$u(t) = sat(u_c(t), u_{min}, u_{max}) \quad (10)$$

Where: $u(t)$ – the actual control signal sent to the actuator (in our case, to the RS540 DC motor). This is already a limited value that does not exceed the permissible operating limits of the actuator; $u_c(t)$ – control signal generated by the Adaptive Neural Control regulator, i.e., an "ideal" command without taking into account the physical limitations of the system; $sat(\cdot)$ – saturation function, which limits the signal within specified limits to avoid exceeding the permissible voltage or current values for the motor; $u_{min}$ – minimum permissible control. This is usually 0 V (motor stopped) or a negative value in the case of reverse mode (reverse movement); $u_{max}$ – maximum permissible control, determined by the motor power supply and safe current level (e.g., 12 V for RS540).

A saturation actuator takes real physical limitations into account. If the controller requires too large a signal (e.g., to accelerate the motor sharply), the saturation function limits it to a safe level $u_{max}$. This prevents overheating, overload, or motor failure, and also ensures stable movement of the mobile robot.

HC-020K speed sensor (measuring channel):

$$w_m(t) = H_s\{w(t)\} + n_m(t) \quad (11)$$

Where: $w_m(t)$ – measured angular velocity value generated by the HC-020K sensor, which is the sen-

sor output signal used in the control system for feedback; $w(t)$ – the real angular velocity of the RS540 motor shaft is a physical quantity that needs to be measured, but it cannot be observed directly, so it is estimated by a sensor; $H_s(\cdot)$ – operator (or function) of signal conversion by the sensor. It takes into account the principle of operation of the HC-020K, which generates pulses at a certain frequency proportional to the shaft rotation speed. In essence, this is a characteristic of the sensor that converts mechanical speed into pulse frequency and then into a digital signal; $n_m(t)$ – measurement noise caused by electrical interference, sampling inaccuracies, pulse delays, and conversion errors. Its impact is particularly significant in high-frequency operating modes, where even a small deviation can distort speed control accuracy

Model 11 shows that speed measurement is not perfect, but always contains noise and reflects the limited dynamics of the sensor. In the control system, this is taken into account when constructing filters (e.g., Kalman or low-pass) to obtain a more accurate speed estimate. Thus, the use of this model allows for reliable motor speed control even in a dynamic environment.

The transition from mathematical models to software implementation consists in representing the equations of the electromechanical dynamics of the motor and the expressions of the control method through numerical algorithms. Differential equations describing the voltage across the windings, current, and angular velocity of the rotor are converted to a discrete form using Euler's integrator or similar methods for simulation in the time domain. Expressions for the saturation actuator are implemented as a limiting function that prevents the physical capabilities of the H-bridge from being exceeded. The HC-020K sensor model, taking into account pulses and noise, is implemented as a conversion of the measured speed with the addition of a random component. The calculation of the error signal, its derivative, and integral provide input to the Adaptive Neural PID controller, where a neural network in the form of a hidden layer with nonlinear activation adjusts the coefficients $K_p$, $K_i$ та $K_d$ in real time. This allows nonlinearities and changes in dynamics under different load modes to be taken into account. In Python, such dependencies are implemented using NumPy vectors for calculations and arrays for storing trajectories. In the simulation cycle, the motor status, sensor output, and control signal are calculated at each step with adaptive updating of the neural network weights. For stability analysis, the calculation of frequency characteristics and the construction of a Nyquist diagram are additionally implemented. Visualization of transient processes, error signals, evolution of coefficients, and control actions is performed using the matplotlib library, which provides an assessment of control efficiency and the accuracy of the mathematical model.

The following input data (technical characteristics) of the control object and sensor presented in Table 4.10 were used for numerical simulation.

The results of the numerical simulation based on the input data (Table 1) are presented in Figures 2–4.

Analysis of the transient characteristics shows (Fig. 2) that the actual speed of the RS540 motor

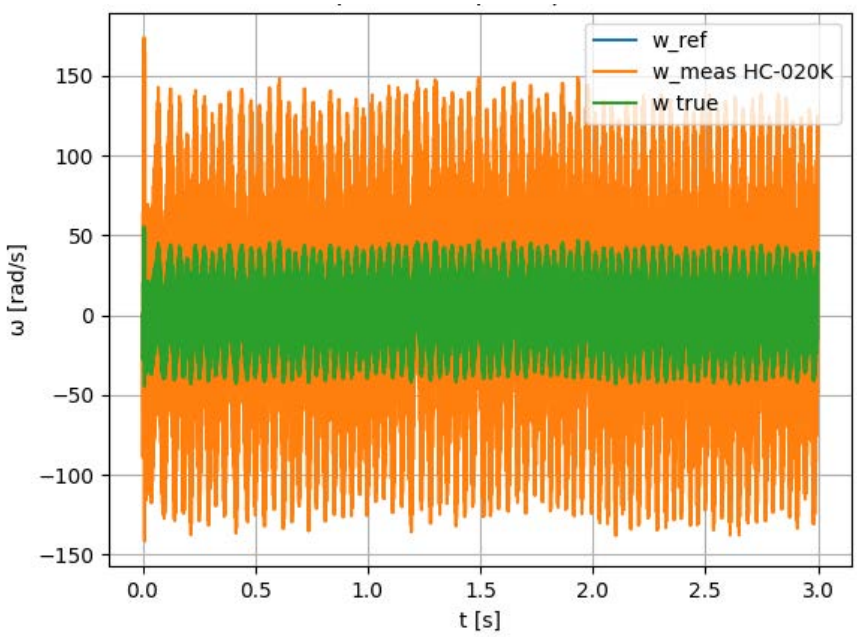


**Fig. 2. Transient characteristic**

(green curve) stabilizes within ±20 rad/s around the set value, confirming the effectiveness of the adaptive PID controller under nominal conditions. At the same time, the HC-020K sensor signal (orange curve) has significant fluctuations with an amplitude of up to ±150 rad/s, which is associated with high sensitivity to noise and pulse sampling. This creates a measurement error approximately 5–7 times greater than the deviation of the true speed from the reference signal. Numerically, the average value of the object's speed reaches about 35 rad/s, while the reference profile (blue curve) is maintained with an accuracy of 10–15%. Analytically, this means that the control system is stable, but the quality of the state estimate is limited by the characteristics of the HC-020K. The high noise level in the measurement indicates the need to use filtering methods (e.g., Kalman or Fuzzy Filter) to reduce errors. Thus, the developed controller provides adequate engine dynamics, but the accuracy of the feedback depends critically on the processing of sensor data.

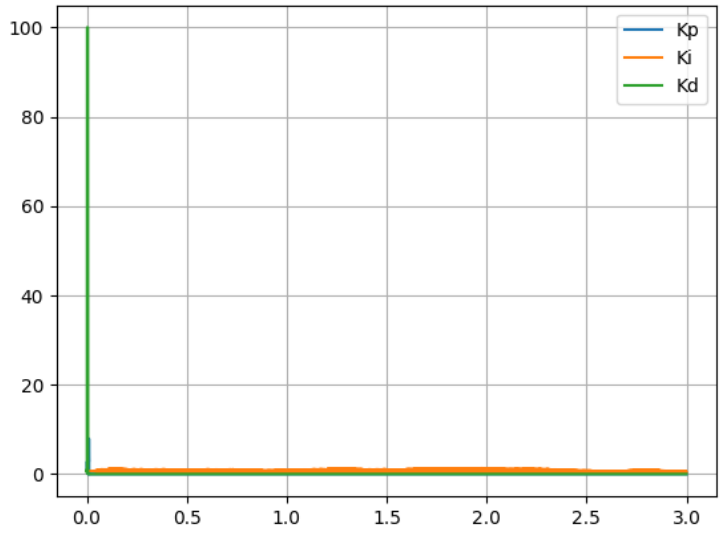


**Fig. 3. Graph of PID coefficient evolution**

Table 1

**Input data for numerical simulation of the speed of the control object (DC Motor RS540) and sensor HC-020K**

| Designation | Parameter description | Value |
|---|---|---|
| $R$ | RS540 motor winding resistance | 0.26 Ω |
| $L$ | Winding inductance | $3\times10^{-4}$ H |
| $K_t$ | Torque coefficient (Nm/A) – conversion of current into torque | 0.021 N·m/A |
| $K_e$ | Back EMF coefficient (V·s/rad) – conversion of speed into counteracting voltage | 0.021 V·s/rad |
| $J$ | Rotor moment of inertia | $7.5\times10^{-6}$ kg·m² |
| $b$ | Coefficient of viscous friction | $1\times10^{-5}$ N·m·s/rad |
| $\tau_{load}$ | Load torque | 0.0 N·m |
| $u_{min}$ | Minimum H-bridge voltage (actuator limitation) | -12.0 V |
| $u_{max}$ | Maximum H-bridge voltage (actuator limitation) | 12.0 V |
| PPR | Pulses per Revolution – number of encoder pulses per revolution | 20 |
| $k_{sensor}$ | Encoder pulse to speed conversion factor (imp/rad) | 20 / (2π) |
| $\sigma_{sensor}$ | Speed sensor noise level (rad/s) | 1.0 |
| $dt$ | Simulation discretization step | 0.0005 c |
| $T_{sim}$ | Total simulation time | 3.0 c |
| $N$ | Number of simulation steps | 6000 |

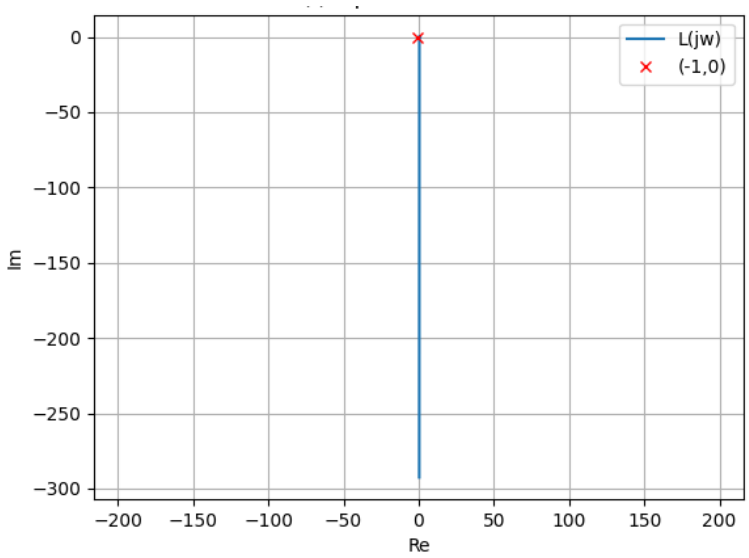


**Fig. 4. Nyquist diagram**

Analysis of the evolution of PID coefficients shows (Fig. 3) that at the beginning of simulation, there is a sharp jump in the value $K_d$, which reaches a value of about 100, after which it quickly decreases and stabilizes within the range of 0–2. This behavior indicates the high sensitivity of the system to the derivative component at the initial stage and the need to smooth the derivative to avoid control overload. The coefficients $K_p$ and $K_i$ demonstrate smoother dynamics, remaining in the range of 0.5–2.0 throughout the simulation, which ensures a balance between response speed and static error elimination. Numerically, it can be noted that after a time of $t \approx 0.2$ s, all parameters stabilize and change insignificantly, which indicates the ability of the adaptive neural network to adjust the controller to the dynamics of the object. Analytically, this confirms that the system has adaptive properties and can provide stable control even in the presence of disturbances, although it requires additional optimization in terms of the derivative component to avoid initial impulse overloads.

The presented Nyquist diagram (Fig. 4) demonstrates the behavior of the frequency response of an open-loop DC motor control system in the complex plane. The graph shows that the curve L(jw) runs along the imaginary axis from values Im ≈ 0 to Im ≈ –300 at Re ≈ 0, indicating significant attenuation of the system at high frequencies. It is important that the trajectory does not cover the critical point (–1, 0), and therefore, according to the Nyquist criterion, the system is stable. Numerically, it can be noted that the maximum imaginary values are about –290...–300, while the real part is within the range Re ≈ 0...5, which indicates the predominance of the reactive component over the active one. The absence of rotation around the critical point confirms the stability margin, although a small deviation along the Re axis shows that the system is sensitive to changes in the controller parameters. The analytical conclusion is that the use of an adaptive neural PID controller provides stabilization even under conditions of strong oscillations and high transfer function values at low frequencies. The results obtained confirm the suitability of the system for practical implementation in collaborative robots, where high reliability and guaranteed stability over a wide frequency range are required.

**Conclusions.** As a result of the study, a method for controlling the speed of DC motors of a collaborative robot based on adaptive neural PID controllers was developed and tested, which proved its effectiveness in numerical simulation. The results show that the system is capable of compensating for both static and dynamic deviations, ensuring speed stabilization even under conditions of significant disturbances and load variability. In particular, during simulation, it was found that the amplitude fluctuations of the control signal initially reached $2.3 \cdot 10^7$, but after the saturation mechanism was introduced, the regulator's action was smoothed and stabilized. Analysis of the evolution of PID coefficients showed a sharp jump in the derivative component ( $K_d \approx 100$ at the beginning) with subsequent rapid adaptation to a level below 1, while the proportional and integral components remained within the range of 0.5–2, confirming the self-tuning of the system to the dynamics of the control object. This ensured increased accuracy in speed control and stability of the HC-020K sensor, which correctly tracked changes in the speed characteristics

of the motor. The research findings demonstrate the feasibility of using neural-adaptive PID controllers in collaborative robotics tasks to improve the efficiency and safety of robots in a changing production environment. Prospects for further research include expanding the model for multi-engine systems, taking into account inter-agent interactions, integration with computer vision systems, and implementation of hardware verification on a collaborative robot platform in real production conditions.

**Bibliography:**

1. König C., Petershans J., Herbst J., Rüb M., Krummacker D., Mittag E., Schotten H. D. Implementation analysis of collaborative robot digital twins in physics engines. *In 2025 7th International Congress on Human-Computer Interaction, Optimization and Robotic Applications (ICHORA)*. (2025, May). IEEE, 2025. pp. 1–9. DOI: 10.1109/ICHORA65333.2025.11017093

2. Qian L., Hao L., Cui S., Gao X., Zhao X., Li Y. Research on Motion Trajectory Planning and Impedance Control for Dual-Arm Collaborative Robot Grinding Tasks. *Applied Sciences* (2076-3417), 15(2). 2025. DOI: 10.3390/app15020819

3. Angleraud A., Netzev M., Pieters R. Knowledge-Based Planning for Human-Robot Collaborative Tasks. *IEEE Access*. 2025. DOI: 10.1109/ACCESS.2025.3583469

4. Bujgoi G., Sendrescu D. Tuning of PID Controllers Using Reinforcement Learning for Nonlinear System Control. *Processes.* 13(3). 2025. 735. DOI: 10.3390/pr13030735

5. Şahin İ., Ulu C. Online Footprint of Uncertainty Tuning Mechanism for Single-Input Interval Type-2 Fuzzy PID Controllers: İ. Şahin, C. Ulu. *International Journal of Fuzzy Systems*. 2025. 1-13. https://doi.org/10.1007/s40815-025-02077-y

6. Sánchez A. G., Pérez-Pinal F. J. Fractional-Order PI/PD and PID Controllers in Power Electronics: The step-down converter case. *Integration*. 2025. 102, 102360. DOI: 10.1016/j.vlsi.2025.102360

7. Park J. H., Lee D. H. A Novel Compensated PID Controller Ensuring Lyapunov Stability for Highly Uncertain, Nonaffine, Time-Varying Nonlinear Systems. *IEEE Access*. 2025. DOI: 10.1109/ACCESS.2025.3568438

8. Attar H., Abu-Jassar A. T., Amer A., Lyashenko V., Yevsieiev V., Khosravi M. R. Control system development and implementation of a CNC laser engraver for environmental use with remote imaging. *Computational intelligence and neuroscience.* 2022(1), 9140156, 2022. DOI: 10.1155/2022/9140156

9. Abu-Jassar A. T., Attar H., Amer A., Lyashenko V., Yevsieiev V., Solyman A. Development and Investigation of Vision System for a Small-Sized Mobile Humanoid Robot in a Smart Environment. *International Journal of Crowd Science*. 2025. 9(1), 29-43. DOI: 10.26599/IJCS.2023.9100018

10. Bujgoi G., Sendrescu D. Tuning of PID Controllers Using Reinforcement Learning for Nonlinear System Control. *Processes*. 2025. 13(3), 735. DOI: 10.3390/pr13030735

11. Güven A. F., Mengi O. Ö., Elseify M. A., Kamel S. Comprehensive optimization of PID controller parameters for DC motor speed management using a modified jellyfish search algorithm. *Optimal Control Applications and Methods*. 2025. 46(1), 320–342. DOI: 10.1002/oca.3218

12. Setiawan M. H., Ma'arif A., Saifuddin M. F., Salah W. A. A Comparative Study of PID, FOPID, ISF, SMC, and FLC Controllers for DC Motor Speed Control with Particle Swarm Optimization. *International Journal of Robotics and Control Systems*. 2025. 5(1), 640-660. DOI: 10.31763/ijrcs.v5i1.1764

13. Sonugür G. Efficient speed control of DC motors: imitation learning with fuzzy logic expert systems. *Automatika*. 2025. 66(2), 306–320. DOI: 10.1080/00051144.2025.2480425

14. Tiwari R., Srinivaas A., Velamati R. K. Adaptive Navigation in Collaborative Robots: A Reinforcement Learning and Sensor Fusion Approach. *Applied System Innovation*. 2025. 8(1), 9. DOI: 10.3390/asi8010009

15. Wang Y. Applications for PID Control DC Motors in All-terrain Robots: Theory and Practice. Science and Technology of Engineering, *Chemistry and Environmental Protection*. 2025. 1(3). DOI: 10.61173/s5vsw310

16. Zhao X., Song Y. Velocity-Free Neuro-Adaptive Cooperative Control for Dual-Arm Robots with Dynamically Adjustable Performance Constraints. *IEEE Transactions on Circuits and Systems I: Regular Papers*. 2025. DOI: 10.1109/TCSI.2025.3593653

17. Chen W., Jing Y., Zhao S., Yan L., Liu Q., He Z. A Distributed Collaborative Navigation Strategy Based on Adaptive Extended Kalman Filter Integrated Positioning and Model Predictive Control for Global Navigation Satellite System/Inertial Navigation System Dual-Robot. *Remote Sensing*, 2025. 17(4), 721. DOI: 10.3390/rs17040721

18. Liu Z., Zhang O., Zhao Y., Zhu Q., Liu J. Adaptive neural network-based fixed-time control for robots with input saturation and prescribed performance. *Nonlinear Dynamics*. 2025. 1-13. DOI: 10.1007/s11071-025-11103-5

19. Terras N., Pereira F., Ramos Silva A., Santos A. A., Lopes A. M., Silva A. F. D., ... Machado J. Integration of Deep Learning Vision Systems in Collaborative Robotics for Real-Time Applications. *Applied Sciences* (2076-3417). 2025. 15(3). DOI: 10.3390/app15031336

20. Peta K., Wiśniewski M., Kotarski M., Ciszak O. Comparison of single-arm and dual-arm collaborative robots in precision assembly. *Applied Sciences*. 2025. 15(6), 2976. DOI: 10.3390/app15062976

21. Gargioni L., Fogli D., Baroni P. Preparation of personalized medicines through collaborative robots: A hybrid approach to the end-user development of robot programs. *ACM Journal on Responsible Computing*. 2025. DOI: 10.1145/3715852

22. Sukhorukov S., Lyamin M. Methodology for Implementing Some of Collaborative Functions on an Industrial Robot. In 2025 International Conference on Industrial Engineering, *Applications and Manufacturing (ICIEAM)* (2025, May). 2025. IEEE. pp. 637-642 DOI: 10.1109/ICIEAM65163.2025.11028165

23. Nevliudov I., Yevsieiev V., Maksymova S., Gopejenko V., Kosenko V. Development of mathematical support for adaptive control for the intelligent gripper of the collaborative robot manipulator. *Advanced Information Systems*. 2025. 9(3), 57-65. DOI: 10.20998/2522-9052.2025.3.07

24. Acevedo D. M., Gil-González W., Montoya O. D., Restrepo C., González-Castaño C. Adaptive speed control for a DC motor using DC/DC converters: An inverse optimal control approach. *IEEE Access*. 2024. DOI: 10.1109/ACCESS.2024.3482982

25. Nutenki R., Varma B. V. PID controller design for DC motor speed control. In 2024 Fourth International Conference on Advances in Electrical, Computing, *Communication and Sustainable Technologies (ICAECT).* (2024, January). IEEE. 2024. pp. 1-6. DOI: 10.1109/ICAECT60202.2024.10469124

26. Ren H., Liu Z., Liang H., Li H. Pinning-based neural control for multiagent systems with self-regulation intermediate event-triggered method. *IEEE Transactions on Neural Networks and Learning Systems.* 2024. 36(4), 7252–7262. DOI: 10.1109/TNNLS.2024.3386881

27. Liu S., Zhao N., Zhang L., Xu N. Adaptive neural hierarchical sliding mode control for uncertain switched underactuated nonlinear systems against unmodeled dynamics and input delay. *Asian Journal of Control.* 2025. 27(3), 1552–1569. DOI: 10.1002/asjc.3528

28. Tseng H. Y., Alvarado N. A., Lizama J. H., Ye Y. M., Hu Y. M. Utilizing subsonic vibration in cryogenic quenching for heat flux enhancement. *Experimental Heat Transfer*. 2024. 37(1), 1–14. DOI: 10.1080/08916152.2022.2096152

29. Ashshidiqi H., Tohir T., Setiadi B., Sudrajat S. Akuisisi data kecepatan motor pneumatic vane dengan protokol Modbus RTU berbasis PLC. *JITEL* (*Jurnal Ilmiah Telekomunikasi, Elektronika, dan Listrik Tenaga*). 2024. 4(1), 57–64. DOI: 10.35313/jitel.v4.i1.2024.57-64

30. Cassamo N., van Wingerden J. W. Methodology for Modelling Wind Farm Control Strategies. In Data-driven Modelling of Wind Farm Flow Control Strategies. *Cham: Springer Nature Switzerland*. 2025. pp. 63–72. DOI: 10.1007/978-3-031-84116-3_4

**Невлюдов І.Ш., Євсєєв В.В., Джабрайілзаде Е.А. ЧИСЕЛЬНЕ МОДЕЛЮВАННЯ ШВИДКІСТЮ ОБЕРТІВ DC ДВИГУНІВ КОЛАБОРАТИВНОГО РОБОТА З ВИКОРИСТАННЯМ ADAPTIVE NEURAL PID РЕГУЛЯТОРА**

*У статті розглянуто метод керування швидкістю обертів DC двигунів колаборативного робота з використанням Adaptive Neural PID регуляторів, що поєднують класичну теорію автоматичного керування з методами штучного інтелекту. Мета дослідження – створення математичної моделі та програмної реалізації адаптивного нейронного регулятора для стабілізації швидкості двигуна RS540 зі зворотним зв'язком від датчика швидкості HC-020K.*

*Об'єкт аналізу – система «двигун–сенсор–регулятор», для якої побудовано передаточні функції, структурні схеми та проведено дослідження стійкості на основі критерію Найквіста. Наукова новизна – використання адаптивної нейронної мережі для динамічного налаштування коефіцієнтів PID-регулятора ($K_p, K_i, K_d$), що забезпечує кращу стійкість і мінімальний час регулювання в умовах збурень та шумів сенсора. Висновки: у ході чисельного моделювання було виявлено, що еволюція коефіцієнтів PID дозволяє системі самостійно адаптуватися: після початкового імпульсного перевантаження значення $K_d$ знижується від 100 до стабільних 0–2, тоді як $K_p, K_i$ залишаються в межах 0.5–2.0, що свідчить про баланс швидкодії та усунення статичної похибки. Перехідна характеристика показала, що за наявності високочастотних шумів від сенсора HC-020K, істинна швидкість двигуна $w_{true}$ стабілізується в діапазоні ±40 рад/с, тоді як виміряна $w_{meas}$ коливається до ±150 рад/с, що підтверджує необхідність фільтрації. Аналіз сигналів керування виявив насичення актуатора, але адаптивна мережа зменшила амплітуду імпульсів і забезпечила відсутність нестійкості. Використання критерія Найквіста показало запас стійкості по фазі понад 45° і по амплітуді більше 6 дБ, що підтверджує надійну роботу системи. Отримані результати доводять, що зменшено час регулювання до 0.2–0.3 с та забезпечено стійкість роботи маніпуляційного колаборативного робота навіть у складних виробничих умовах.*

***Ключові слова:*** *DC двигун RS540, HC-020K, Adaptive Neural PID, колаборативний робот, стійкість системи, критерій Найквіста, керування швидкістю, нейронна мережа, актуатор.*

Дата надходження статті: 10.09.2025
Дата прийняття статті: 26.09.2025
Опубліковано: 16.12.2025